Journal of Organometallic Chemistry 867 (2018) 208–213

Contents lists available at ScienceDirect

Journal of Organometallic Chemistry

journal homepage: www.elsevier.com/locate/jorganchem

Sterically encumbered dianionic dicarboranyl pincer ligand $(C_5H_3N)(C_2B_{10}H_{11})_2$ and its CNC Nickel(II) complex

Mohammad Jahirul Islam, Mark D. Smith, Dmitry V. Peryshkov*

Department of Chemistry and Biochemistry, University of South Carolina, 631 Sumter Street, Columbia, SC 29208, USA

ARTICLE INFO

Article history:
Received 10 October 2017
Received in revised form
3 November 2017
Accepted 5 November 2017
Available online 7 November 2017

This paper is dedicated to professor Irina P. Beletskaya on the occasion of her 85th birthday.

Keywords:
Carboranes
Pincer complexes
Nickel

ABSTRACT

The novel 2,6-bis(carborane)pyridine $(C_5H_3N)(C_2B_{10}H_{11})_2$ ligand precursor containing two icosahedral carborane clusters attached to the pyridine ring was synthesized by the S_NAr reaction between 2,6-difluoropyridine and lithiated *ortho*-carborane $LiC_2B_{10}H_{11}$. Lithiation of the proligand at carbon atoms of carborane cages and the subsequent reaction with $Ni(PPh_3)_2Cl_2$ afforded the square-planar Ni(II) pincer complex $\{(C_5H_3N)(C_2B_{10}H_{10})_2\}Ni(CH_3CN)$. X-ray single crystal diffraction revealed extreme steric hindrance around the metal center in the complex imposed by two carboranyl groups in the rigid pincer-type framework, which was also manifested by the high value of the ligand buried volume $\%V_{bur} = 70.6\%$. The title pincer complex $\{(C_5H_3N)(C_2B_{10}H_{10})_2\}Ni(CH_3CN)$ was found to be a competent catalyst for nucleophilic addition of piperidine to acetonitrile.

1. Introduction

Pincer-type frameworks, which are tridentate ligands that enforce meridional coordination to a metal center, attracted significant attention in last 20 years [1]. Pincer complexes of transition metals often exhibit a favorable combination of both stability and reactivity, which made them invaluable for fundamental studies of reaction mechanisms and for catalysis. As originally devised by Moulton and Shaw, pincer ligands contain an anionic carbon center between two pendant phosphine donors "arms" [2]. This arrangement type has been broadened to include other monoanionic moieties with two neutral sterically hindered arms and it is the most studied subclass of pincer ligands [3]. Related dianionic and trianionic pincer-type ligands and their complexes with both early- and late transition metals have recently attracted increased attention [4–8].

Icosahedral boron clusters, such as neutral *closo*-carboranes $C_2B_{10}H_{12}$ and their monoanionic counterparts $CB_{11}H_{\bar{1}2}$ possess an unusual delocalized electronic structure as well as an extreme steric hindrance profile that make them interesting building blocks in ligand design, catalysis, polymer and material chemistry [9–16]. Carboranes have been used as auxiliary groups attached to phosphines, amines, amides, cyclopentadienyls, and heterocyclic carbene systems [17–23].

A number of tridentate complexes containing carboranes has recently emerged [24–27]. The utilization of the pincer-type geometry with boron cages serving as central "backbones" allowed, for example, an isolation of an unusual three-membered (BB)>Ru carboryne metalacycle [28] as well as a development of an efficient, water-tolerant Pd-based catalyst for Suzuki coupling reactions [26] and an air-tolerant Ru-based catalyst for alkane transfer dehydrogenation [29].

In general, carborane clusters can be exohedrally metalated at carbon or boron vertices. The C–H bonds of carboranes are relatively acidic ($pKa = 22$ for *ortho*-carborane), and these C atoms can be lithiated and subsequently transmetalated by transition metal salt metathesis [30–35]. In contrast, unsupported metal-boron bonds of carboranes are rare [36–39]. However, there are numerous examples of successful metalation of carborane B–H bonds, primarily by late transition metals, with the use of donor directing groups attached to the cage. These cyclometalated products are intermediates in direct selective B-H bond functionalization of boron clusters and often are isolable [40–46].

In this contribution, we report the synthesis of the novel type of the chelating pincer ligand precursor containing *two* sterically

* Corresponding author.
E-mail address: peryshkov@sc.edu (D.V. Peryshkov).

https://doi.org/10.1016/j.jorganchem.2017.11.004
0022-328X/

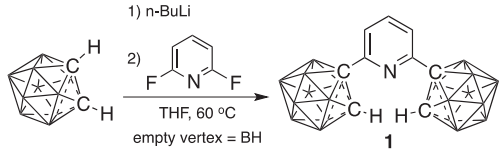

Scheme 1. Synthesis of 2,6- bis(carborane)pyridine (C_5H_3N)($C_2B_{10}H_{11}$)$_2$ (**1**).

hindered icosahedral carborane cages as "arms" and a pyridine "backbone". Deprotonation of C-H bonds of both carborane clusters afforded a dianionic ligand that was successfully metalated to yield a nickel(II) complex.

2. Results and discussion

The use of carborane clusters as "arms" of a pincer ligand prompts the use of a neutral donor as a central "backbone". The rigidity of the target pincer ligand was an important consideration, therefore, we chose not to use carborane picolyl derivatives where a boron cluster is connected to a pyridine ring through the methylene linker [47–49]. Instead, we elected to use a rigid planar pyridine fragment as its direct functionalization with two carborane cages in 2- and 6- positions would lead to meridional geometry of the target ligand. Several synthetic routes to carboranyl pyridines have been reported in literature, including reactions of decaborane and pyridyl acetylenes and copper-promoted coupling of 2-bromopyridine and lithiated carborane [50–52]. These synthetic methods, while successful, have been plagued by relatively low yields. Recently, a simpler alternative method, involving nucleophilic aromatic substitution of 2-fluoropyridine by lithiated carborane, has been developed [53]. Notably, all these previously reported synthetic routes led to pyridine derivatives containing one carborane cage. We surmised that the S_NAr reaction of 2,6-difluoropyridine with two equivalents of lithiated carborane would lead to efficient formation of the dicarboranyl pyridine. Gratifyingly, heating the mixture of 2,6-difluropyridine with $LiC_2B_{11}H_{11}$ in THF at 80 °C under nitrogen atmosphere overnight led, after aqueous workup and extraction to dichloromethane, to the target 2,6-dicarboranyl pyridine (C_5H_3N)($C_2B_{10}H_{11}$)$_2$ (**1**) (see Scheme 1). The product was characterized by the array of multinuclear NMR spectrometry techniques, mass-spectrometry, and the single crystal X-ray diffraction. The ^{11}B and $^{11}B\{^1H\}$ NMR spectra of **1** exhibited a set partially overlapping signals in the range from -2.6 to -13.1 ppm. The ^1H NMR resonance corresponding to the remaining C-H bond of the carborane cage was found at 4.49 ppm in $CDCl_3$, which is shifted downfield in comparison with the related signal of the starting $C_2B_{10}H_{12}$ cluster at 3.56 ppm.

Single crystals of **1** were grown from dichloromethane/hexanes solvent mixture by slow evaporation on air. The structure determination confirmed the expected geometry of the proligand with crystallographically-required C_2 and idealized C_{2v} symmetry (see Fig. 1). The central pyridine fragment is connected to carborane cages through unstrained bonds with the C2–C3 bond length of 1.496(3) Å, the N1–C3–C2 angle of 116.6(2)° and the C3–C2–C1 angle of 117.5(2)°. The C1–C2 bond in the carborane cluster is 1.629(2) Å. The separation between two boron cages is substantial as indicated by the C1···C1A distance of 4.554(3) Å.

Interestingly, the molecular structure of **1** in the solid state revealed a conformation that features C–H bonds of carborane clusters pointing inwards the cavity of the ligand, in other words, towards the nitrogen atom of the pyridine ring. This arrangement is likely stabilized by the intramolecular C–H···N hydrogen bonding which has been found in the related 2-carboranylpyridine [54]. Similarly, existence of relatively strong hydrogen bonds between

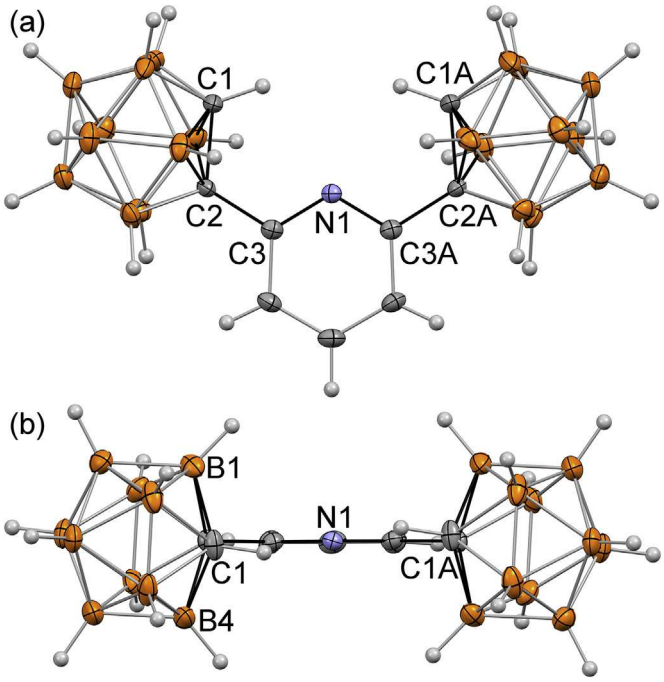

Fig. 1. Displacement ellipsoid plot (50% probability) of the proligand (C_5H_3N)($C_2B_{10}H_{11}$)$_2$ (**1**). (a): a view perpendicular to the (C3–N1–C3A) plane (b): a view along the (C3–N1–C3A) plane.

aryl C–H bonds and nitrogen atoms of pyridines have been demonstrated [55].

The ligand precursor **1** possesses two relatively acidic C-H bonds on two carborane cages. Deprotonation of the ligand was done using 2.1 equiv *n*-BuLi in THF at room temperature. The lithiated ligand was not isolated but used *in situ* in the reaction with 1.1 equiv of $Ni(PPh_3)_2Cl_2$ at 60 °C for 6 h (see Scheme 2). The target complex {(C_5H_3N)($C_2B_{10}H_{10}$)$_2$}Ni(CH_3CN) (**2**) was isolated as a yellow powder.

Single crystals of **2·C$_6$H$_6$** were grown from benzene by slow evaporation. The structure determination revealed the expected square-planar geometry around the nickel center that is coordinated to two carboranyl arms through carbon atoms, the pyridine ring, and acetonitrile. The complex adopted crystallographically-required C_{2v} symmetry, however, elongated displacement ellipsoids of boron atoms suggested mild cluster disorder through their displacement from the mirror plane. The Ni1–C1 bond length in **2** is 1.929(2) Å. This value is within the typical range for nickel *C*-carboranyl compounds (1.880(6)–2.01(1) Å) [56]. The Ni1–N2(C_6H_3) bond length is 1.882(2) Å and the Ni1–N2(CCH_3) bond length is 1.841(2) Å. The C2≡N6 bond length of the coordinated acetonitrile ligand is 1.134(5) Å. The coordination of the metal center led to the increased strain of the complex which is indicated by the decreased intraligand angles N1–C3–C2 (113.4(2)°) and C3–C2–C1 (110.6(2)°). This is also manifested in the decreased separation between boron cages in **2** with the C1···C1A distance of

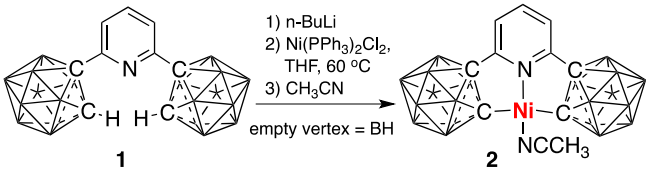

Scheme 2. Synthesis of {(C_5H_3N)($C_2B_{10}H_{10}$)$_2$}Ni(CH_3CN) (**2**).

3.853(3) Å. The C1–Ni1–C1A bite angle is close to linearity at 173.7(1)°.

The diamagnetic complex **2** was characterized by ^{1}H, ^{13}C, and ^{11}B NMR, and FTIR spectroscopies. The FTIR spectrum of the solid sample exhibited characteristic absorption bands ν(B–H) at 2586 cm^{-1} as well as ν(C≡N) at 2332 cm^{-1}. The ^{11}B NMR spectrum contained a set of partially overlapping signals in the range from −3.4 ppm to −11.3 ppm (see Fig. 2).

Carborane clusters as ligands exert an unusually high degree of steric hindrance due to their icosahedral shape. For example, each of the metal-carbon bonds in **2** is surrounded by five neighboring cluster atoms. A space-filling diagram of the complex **2** with acetonitrile ligand omitted is shown in Fig. 2c to highlight steric requirements of 2,6-bis(carborane)pyridine. Ligand buried volume (%V_{bur}) has been recently introduced as a quantitative descriptor of steric congestion around the metal center [57]. We found that the $(C_5H_3N)(C_2B_{10}H_{10})_2$ ligand in the complex **2** exhibited a high value of %V_{bur} = 70.6%, which indicates a high degree of steric hindrance imposed by the dicarboranyl pincer ligand. This value can be compared to that for the recently reported complex of gold featuring two anionic carborane $\{CB_{11}\}$ cages connected to the N-heterocyclic carbene backbone [58]. The presence of five-membered ring NHC backbone as well as two weakly coordinating anionic boron cages in that complex have resulted in the value of %V_{bur} of 47.2%. The neutral $(C_5H_3N)(C_2B_{10}H_{10})_2$ ligand reported herein is pyridine-based, which enforces two neutral $\{C_2B_{10}\}$ carborane cages closer to each other leading to the coordination to the metal center and the increase in %V_{bur}.

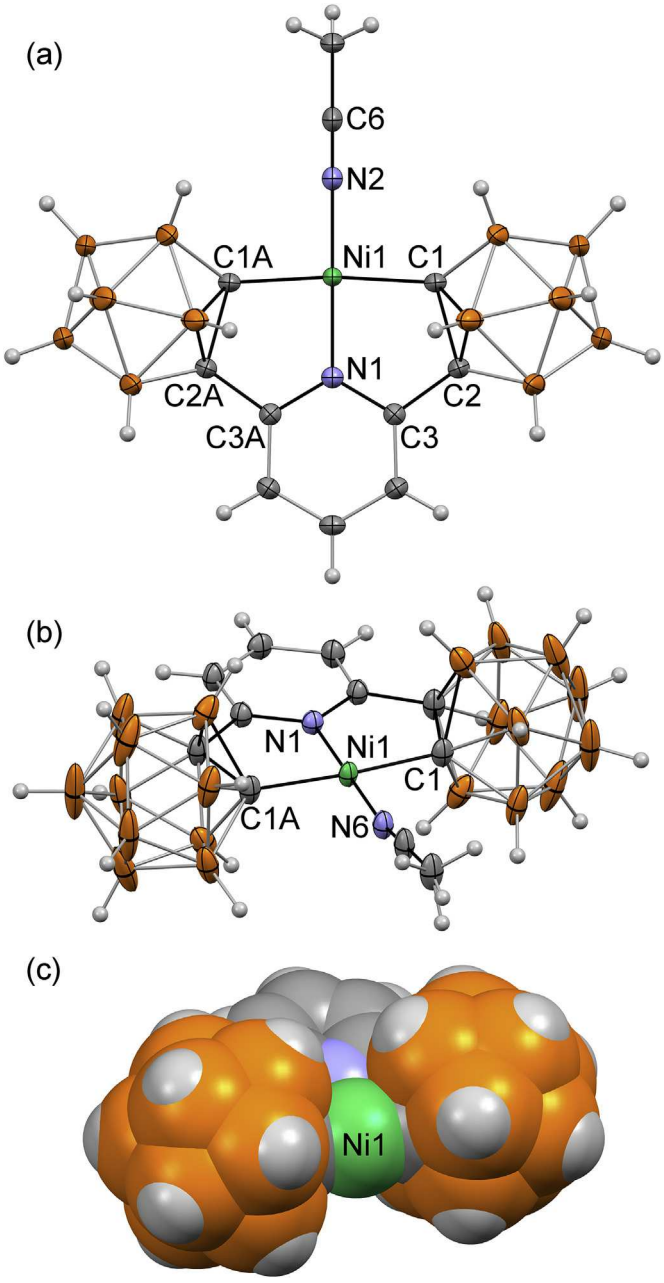

Fig. 2. Displacement ellipsoid plot (50% probability) of the $\{(C_5H_3N)(C_2B_{10}H_{10})_2\}$ Ni(CH_3CN) complex (**2**). (a): a view perpendicular to the (C3–N1–Ni1–C3A) plane (b): a general view (c): space-filling diagram of **2** with the acetonitrile ligand omitted.

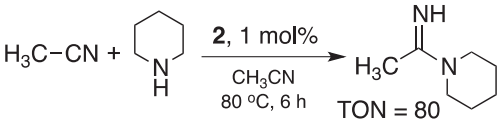

Scheme 3. Addition of piperidine to acetonitrile promoted by **2**. The catalyst loading was 1 mol% relative to the amount of piperdine. Acetonitrile served as both the reagent and the solvent.

The electron density distribution in the carborane cluster is not uniform and gives rise to significant differences in the electronic effects of the carborane cage on an exohedral substituent when attached to either carbon or boron atoms [59]. A carborane cluster is usually regarded as an electron-withdrawing group when it is bound through its carbon atom [60]. The high value of the ν(CN) in **2** indicates the electron-deficient environment of the nitrile group which is likely due to coordination to relatively electron-poor *C*-carboranyl bound metal center. A significant positive charge on the carbon atom of the nitrile group would assist a nucleophilic attack, for example, by an amine. Notably, there have been reports of cationic nickel(II) complexes catalyzing hydroamination of nitriles via an outer-sphere mechanism [61,62].

We found that the complex **2** efficiently catalyzes the addition of piperidine to acetonitrile with the formation of the imine $HN{=}C(CH_3)NC_5H_{10}$. In a typical reaction, a mixture of piperidine and acetonitrile containing **2** (1 mol% relative to the amount of piperidine) was heated at 80 °C for 6 h (Scheme 3). A relatively high value of the turnover number (TON = 80) was observed, thus demonstrating that the complex **2** is a competent catalyst of this reaction.

3. Conclusions

The novel pincer ligand framework containing two carborane clusters and a central pyridine backbone was synthesized. The CNC-type pincer complex 2,6-bis(carboranyl)pyridine nickel(-II)(acetonitrile) was prepared in the reaction of the lithiated ligand $Li_2(C_5H_3N)(C_2B_{10}H_{10})_2$ and $Ni(PPh_3)_2Cl_2$. The molecular structure of the nickel complex featured high degree of steric hindrance imposed by coordination of two icosahedral carborane clusters. The title complex was found to be a competent catalyst for hydroamination of acetonitrile with piperidine.

4. Experimental section

All synthetic manipulations, unless stated otherwise, were carried out either in a nitrogen-filled VAC drybox or on a dual-manifold Schlenk-style vacuum line [63]. The solvents were sparged with nitrogen, passed through activated alumina, and stored over activated 4 Å Linde-type molecular sieves. CD_2Cl_2,

$CDCl_3$, and $(CD_3)_2SO$ were degassed and stored over activated 4 Å Linde-type molecular sieves. NMR spectra were recorded using Varian spectrometers at 400 (^{1}H), 100 (^{13}C), 128 (^{11}B) MHz, reported in δ (parts per million) and referenced to the residual ^{1}H/^{13}C signals of the deuterated solvent or an external $BF_3(Et_2O)$ (^{11}B(δ): 0.0 ppm) standard.

4.1. Synthesis of 2,6-bis(carborane)pyridine $(C_5H_3N)(C_2B_{10}H_{11})_2$ **(1)**

A solution of *n*-butyllithium in hexanes (1.6 M, 3.5 mL, 5.6 mmol) was added to a solution of *ortho*-carborane (400 mg, 2.77 mmol) in 10 mL of anhydrous tetrahydrofuran at room temperature under nitrogen atmosphere. The mixture was stirred at room temperature for 12 h. 2,6-difluoropyridine (0.13 mL, 1.43 mmol) was added to the reaction mixture and stirred at 60 °C for 6 h, after which time tetrahydrofuran was removed under vacuum. Dichloromethane (50 mL) and water (50 mL) were added, and products were extracted to the organic layer. The organic portion was passed through a silica gel column using dichloromethane as an eluent. Volatiles were removed under vacuum and the unreacted *ortho*-carborane was sublimed out to obtain pure 2,6-bis(carborane)pyridine with 28% yield (140 mg, 0.385 mmol).

^{1}H NMR ($CDCl_3$): δ 7.78 (t, 1H, C_5H_3N), 7.63 (d, 2H, C_5H_3N), 4.49 (s, 2H, (C-*H*, $C_2B_{10}H_{11}$), 3.10–1.50 (overlapping, 20H, B-*H*, $C_2B_{10}H_{11}$). **^{11}B{^{1}H} NMR** ($CDCl_3$): δ -2.6, -3.4, -8.3, -11.4, -13.1 (br). **^{13}C NMR** ($CDCl_3$): δ 150.5 (C_5H_3N), 139.2 (C_5H_3N), 122.8 (C_5H_3N), 74.0 (C-*C*, $C_2B_{10}H_{11}$), 56.6 (*C*-H, $C_2H_{11}B_{10}$). Calcd for $C_9H_{27}B_{20}N$: C, 29.57; H, 7.45; N, 3.83 Found: C, 29.38; H, 7.11, N, 3.61.

4.2. Synthesis of 2,6-bis(carboranyl)pyridine nickel(II)(acetonitrile) complex $\{(C_5H_3N)(C_2B_{10}H_{10})_2\}Ni(CH_3CN)$ **(2)**

A solution of *n*-butyllithium in hexanes (1.6 M, 0.72 mL, 1.16 mmol) was added to a solution of 2,6-bis(carborane)pyridine (200 mg, 0.55 mmol) in 10 mL of dry tetrahydrofuran at room temperature under nitrogen. The mixture was stirred at room temperature for 12 h. Bis(triphenylphosphine)nickel(II) dichloride (395.77 mg, 0.61 mmol) was added and the mixture was stirred at 60 °C for 6 h, after which time volatiles were removed under vacuum. Hydrochloric acid (3 M, 20 mL) and acetonitrile (20 mL) were added. The mixture was filtered and the resulting precipitate was washed with hexanes (10 mL) and diethyl ether (10 mL) to obtain 2,6-bis(carboranyl)pyridine nickel(II)(acetonitrile) complex as a yellow powder (89 mg, 0.19 mmol, 35% yield).

^{1}H NMR (CD_2Cl_2): δ 7.79 (t, 1H, C_5H_3N), 7.22 (d, 2H, C_5H_3N), 3.50–1.20 (overlapping, B-*H*, $C_2B_{10}H_{10}$), 2.38 (s, 3H, CH_3CN). **^{11}B{^{1}H} NMR** (CD_2Cl_2): δ -3.4, -6.7, -7.5, -11.3.**^{13}C NMR** (($CD_3)_2SO$): δ 159.7 (C_5H_3N), 143.1 (C_5H_3N), 122.3 (C_5H_3N), 118.7 (CH_3CN), 79.7 ($C_2H_{11}B_{10}$), 71.9 ($C_2H_{11}B_{10}$), 1.7 (CH_3CN). Calcd for $C_{11}H_{26}B_{20}N_2Ni$: C, 28.64; H, 5.68; N, 6.07 Found: C, 28.71; H, 5.80, N, 5.72.

4.3. Hydroamination of acetonitrile promoted by **2**

Piperidine (0.1 mL, 1.0 mmol) was added to a solution of 2,6-bis(carboranyl)pyridine nickel(II)(acetonitrile) complex (**2**) (4.62 mg, 0.01 mmol) in 5 mL of acetonitrile and the reaction mixture was stirred at 80 °C for 6 h. A solution of naphthalene (12.82 mg, 1.0 mmol) in 10 mL of ether was added to the mixture as an internal ^{1}H NMR spectroscopy standard. The volatiles were removed under vacuum at room temperature. The turnover number (TON = 80) was determined by integration of signals corresponding to the imine product relative to signals of the internal standard (naphthalene) in the ^{1}H NMR spectrum of the reaction mixture.

4.4. Structure determination details

The calculations of the buried volume $\%V_{bur}$ were carried out for the atomic coordinates from the crystal structure of **2** using SambVca2 program (https://www.molnac.unisa.it/OMtools/sambvca2.0/) [57] with the following (default) parameters: sphere radius 3.5 Å, distance from the center of the sphere: 2.1 Å, mesh spacing: 0.05 Å, H atoms not included, and Bondi radii scaled by 1.17.

X-ray intensity data from a colorless, almond-shaped plate were collected at 100(2) K using a Bruker D8 QUEST diffractometer equipped with a PHOTON-100 CMOS area detector and an Incoatec microfocus source (Mo Kα radiation, λ = 0.71073 Å). The raw area detector data frames were reduced and corrected for absorption effects using the Bruker APEX3, SAINT+ and SADABS programs [64–66]. Final unit cell parameters were determined by least-squares refinement of large sets of reflections from the data sets. The structure was solved with SHELXT [67,68]. Subsequent difference Fourier calculations and full-matrix least-squares refinement against F^2 were performed with SHELXL-2016 using OLEX2 [69].

4.4.1. Crystal structure determination of $(C_5H_3N)(C_2B_{10}H_{11})_2$ **(1)**

The compound crystallized in the tetragonal system. The pattern of systematic absences in the intensity data was consistent with the space groups *I*-42*d* and *I*4$_1$*md*. Space group *I*-42*d* (No. 122) was confirmed by structure solution. The asymmetric unit consists of half of one molecule, which is located on a crystallographic two-fold axis of rotation. All non-hydrogen atoms were refined with anisotropic displacement parameters. All hydrogen atoms were located in Fourier difference maps and refined freely, resulting in normal bond distances and displacement parameters. The largest residual electron density peak in the final difference map is 0.23 e Å^{-3}, located 0.72 Å from C1. Because of the absence of heavy atoms in the crystal, the absolute structure could not be determined.

Crystal Data for $C_9H_{25}B_{20}N$ (CCDC 1583707): tetragonal, space group I-42d (no. 122), a = 14.9477(5) Å, c = 19.0491(7) Å, V = 4256.2(3) Å3, Z = 8, T = 100(2) K, μ(MoKα) = 0.051 mm-1, M = 363.50 g/mol, D_{calc} = 1.135 g/cm^3, 47566 reflections measured (5.45° ≤ 2Θ ≤ 52.806°), 2188 unique (R_{int} = 0.0700, R_{sigma} = 0.0185) which were used in all calculations. The final R_1 was 0.0401 (I > 2σ(I)) and wR_2 was 0.1047 (all data).

4.4.2. Crystal structure determination of $\{(C_5H_3N)(C_2B_{10}H_{10})_2\}Ni(CH_3CN)(C_6H_6)_2$ $(2\cdot(C_6H_6)_2)$

The compound crystallized in the orthorhombic system. The pattern of systematic absences in the intensity data was consistent with the space groups *Imma* and *Ima*2. The centrosymmetric group *Imma* was eventually confirmed as the best description of the structure. The asymmetric unit consists of ¼ of one Ni complex with crystallographic *mm* (C_{2v}) point symmetry, and half of one benzene molecule located on a mirror plane. Atoms Ni1, N1, C5, N2, C1, C2, B5 and B6 are located in the mirror plane perpendicular to the crystallographic *a* axis; Ni1, N1, C5, N2, C6 and C7 are also located in the mirror perpendicular to the *b* axis. The carbon and hydrogen atoms of the acetonitrile ligand (C6 and C7) are disordered across the mirror perpendicular to the *a* axis and were refined with half-occupancy. The benzene solvent guest disorder consists of two independent half-benzene molecules per asymmetric unit, both located on the mirror plane perpendicular to the *b* axis. All non-hydrogen atoms were refined with anisotropic displacement parameters. The anisotropic displacement parameters (*adps*) of the disordered benzene carbon atoms were restrained to be approximately spherical using an ISOR restraint. Some elongated *adps* for boron atoms in the carborane cage (*e.g.* U_3/U_1 = 11.4 for B6) suggest some atoms in the cage part of the structure are displaced away

from the mirror plane bisecting the cage. A refinement in space group *Ima*2, which still retains this mirror plane, also showed strongly prolate boron *adp*s and was unstable. Refinements in lower space groups without mirror symmetry (*e.g.* $I2_12_12_1$) also gave highly prolate boron ellipsoids and unstable refinements. Disorder modeling in *Imma* of the carborane cage part was not successful owing to the small displacements of the B atoms from their average positions. The best refinement was therefore judged to be in space group *Imma* with prolate boron ellipsoids suggesting mild cage disorder. Hydrogen atoms bonded to carbon were placed in geometrically idealized positions and included as riding atoms with *d*(C-H) = 0.95 Å and *U*iso(H) = 1.2*U*eq(C) for aromatic hydrogen atoms. The acetonitrile methyl hydrogens were located in a difference map, adjusted to *d*(C-H) = 0.98 Å and *U*iso(H) = 1.5*U*eq(C) included as riding on C7. Hydrogen atoms bonded to boron atoms were located in difference maps and refined freely. The largest residual electron density peak in the final difference map is 0.28 e Å^{-3}, located 0.45 Å from B6.

Crystal Data for $C_{23}H_{38}B_{20}N_2Ni$ (CCDC 1583707): orthorhombic, space group *Imma* (no. 74), a = 14.4701(8) Å, b = 16.2302(8) Å, c = 14.0240(7) Å, V = 3293.6(3) Å^3, Z = 4, T = 100(2) K, μ(MoKα) = 0.611 mm^{-1}, M = 617.46 g/mol, D_{calc} = 1.245 g/cm^3, 66111 reflections measured ($5.02^\circ \leq 2\Theta \leq 55.472^\circ$), 2080 unique ($R_{int}$ = 0.0390, R_{sigma} = 0.0109) which were used in all calculations. The final R_1 was 0.0309 ($I > 2\sigma(I)$) and wR_2 was 0.0815 (all data).

Acknowledgments

This material is based in part upon work supported by the National Science Foundation under Award CHE-1654301.

References

[1] G. van Koten, R.A. Gossage (Eds.), The Privileged Pincer-metal Platform: Coordination Chemistry & Applications, first ed., Springer, 2015, 2016 edition.
[2] C.J. Moulton, B.L. Shaw, Transition metal–carbon bonds. Part XLII. Complexes of nickel, palladium, platinum, rhodium and iridium with the tridentate ligand 2,6-bis[(di-t-butylphosphino)methyl]phenyl, J. Chem. Soc. Dalton Trans. (1976) 1020–1024, https://doi.org/10.1039/DT9760001020.
[3] G. van Koten, Tuning the reactivity of metals held in a rigid ligand environment, Pure Appl. Chem. 61 (2009) 1681–1694, https://doi.org/10.1351/pac198961101681.
[4] M.E. O'Reilly, A.S. Veige, Trianionic pincer and pincer-type metal complexes and catalysts, Chem. Soc. Rev. 43 (2014) 6325–6369, https://doi.org/10.1039/C4CS00111G.
[5] A.I. Nguyen, K.J. Blackmore, S.M. Carter, R.A. Zarkesh, A.F. Heyduk, One- and two-electron reactivity of a Tantalum(V) complex with a redox-active tris(amido) ligand, J. Am. Chem. Soc. 131 (2009) 3307–3316, https://doi.org/10.1021/ja808542j.
[6] S. Sarkar, K.P. McGowan, J.A. Culver, A.R. Carlson, J. Koller, A.J. Peloquin, M.K. Veige, K.A. Abboud, A.S. Veige, NCN trianionic pincer ligand precursors: synthesis of bimetallic, chelating diamide, and pincer group iv complexes, Inorg. Chem. 49 (2010) 5143–5156, https://doi.org/10.1021/ic100232s.
[7] S. Sarkar, K.P. McGowan, S. Kuppuswamy, I. Ghiviriga, K.A. Abboud, A.S. Veige, An OCO^{3-} trianionic pincer tungsten(vi) alkylidyne: rational design of a highly active alkyne polymerization catalyst, J. Am. Chem. Soc. 134 (2012) 4509–4512, https://doi.org/10.1021/ja2117975.
[8] A. Sattler, G. Parkin, A new class of transition metal pincer ligand: tantalum complexes that feature a [CCC] X_3-donor array derived from a terphenyl ligand, J. Am. Chem. Soc. 134 (2012) 2355–2366, https://doi.org/10.1021/ja210404x.
[9] M.F. Hawthorne, Boron, my favorite element, J. Chem. Educ. 86 (2009) 1131, https://doi.org/10.1021/ed086p1131.
[10] R.N. Grimes, Carboranes in the chemist's toolbox, Dalton Trans. 44 (2015) 5939–5956, https://doi.org/10.1039/C5DT00231A.
[11] N.S. Hosmane (Ed.), Boron Science: New Technologies and Applications, 1 edition, CRC Press, Boca Raton. FL, 2011.
[12] R.N. Grimes, Carboranes, third ed., Academic Press, Amersterdam; Boston, 2016, 3rd edition.
[13] B.P. Dash, R. Satapathy, J.A. Maguire, N.S. Hosmane, Polyhedral boron clusters in materials science, New J. Chem. 35 (2011) 1955–1972, https://doi.org/10.1039/C1NJ20228F.
[14] C. Douvris, J. Michl, Update 1 of: chemistry of the carba-closo-dodecaborate(−) anion, $CB_{11}H_{\bar{1}2}$, Chem. Rev. 113 (2013) PR179–PR233, https://doi.org/10.1021/cr400059k.
[15] G. Chen, J. Yang, G. Lu, P.C. Liu, Q. Chen, Z. Xie, C. Wu, One stone kills three birds: novel boron-containing vesicles for potential BNCT, controlled drug release, and diagnostic imaging, Mol. Pharm. 11 (2014) 3291–3299, https://doi.org/10.1021/mp400641u.
[16] R. Núñez, I. Romero, F. Teixidor, C. Viñas, Icosahedral boron clusters: a perfect tool for the enhancement of polymer features, Chem. Soc. Rev. 45 (2016) 5147–5173, https://doi.org/10.1039/C6CS00159A.
[17] A.R. Popescu, F. Teixidor, C. Viñas, Metal promoted charge and hapticities of phosphines: the uniqueness of carboranylphosphines, Coord. Chem. Rev. 269 (2014) 54–84. https://doi.org/10.1016/j.ccr.2014.02.016.
[18] Z.-J. Yao, G.-X. Jin, Transition metal complexes based on carboranyl ligands containing N, P, and S Donors: synthesis, reactivity and applications, Coord. Chem. Rev. 257 (2013) 2522–2535, https://doi.org/10.1016/j.ccr.2013.02.004.
[19] N. Fey, M.F. Haddow, R. Mistry, N.C. Norman, A.G. Orpen, T.J. Reynolds, P.G. Pringle, Regioselective B-Cyclometalation of a bulky o-carboranyl phosphine and the unexpected formation of a dirhodium(ii) complex, Organometallics 31 (2012) 2907–2913, https://doi.org/10.1021/om201198s.
[20] A.M. Spokoyny, C.D. Lewis, G. Teverovskiy, S.L. Buchwald, Extremely electron-rich, boron-functionalized, icosahedral carborane-based phosphinoboranes, Organometallics 31 (2012) 8478–8481, https://doi.org/10.1021/om301116x.
[21] A. El-Hellani, V. Lavallo, Fusing N-Heterocyclic carbenes with carborane anions, Angew. Chem. Int. Ed. 53 (2014) 4489–4493, https://doi.org/10.1002/anie.201402445.
[22] J. Estrada, V. Lavallo, Fusing dicarbollide ions with N-Heterocyclic carbenes, Angew. Chem. Int. Ed. 56 (2017) 9906–9909, https://doi.org/10.1002/anie.201705857.
[23] J. Holmes, C.M. Pask, M.A. Fox, C.E. Willans, Tethered N-heterocyclic carbene–carboranes: unique ligands that exhibit unprecedented and versatile coordination modes at rhodium, Chem. Commun. 52 (2016) 6443–6446, https://doi.org/10.1039/C6CC01650B.
[24] A.M. Spokoyny, M.G. Reuter, C.L. Stern, M.A. Ratner, T. Seideman, C.A. Mirkin, Carborane-based pincers: synthesis and structure of SeBSe and SBS Pd(II) complexes, J. Am. Chem. Soc. 131 (2009) 9482–9483, https://doi.org/10.1021/ja902526k.
[25] M.E. El-Zaria, H. Arii, H. Nakamura, m-Carborane-Based chiral NBN pincer-metal complexes: synthesis, structure, and application in asymmetric catalysis, Inorg. Chem. 50 (2011) 4149–4161, https://doi.org/10.1021/ic2002095.
[26] M.Y. Tsang, C. Viñas, F. Teixidor, J.G. Planas, N. Conde, R. SanMartin, M.T. Herrero, E. Domínguez, A. Lledós, P. Vidossich, D. Choquesillo-Lazarte, Synthesis, structure, and catalytic applications for ortho- and meta-carboranyl based NBN Pincer-Pd complexes, Inorg. Chem. 53 (2014) 9284–9295, https://doi.org/10.1021/ic5013999.
[27] B.J. Eleazer, M.D. Smith, D.V. Peryshkov, Metal- and ligand-centered reactivity of meta-carboranyl-backbone pincer complexes of rhodium, Organometallics 35 (2016) 106–112, https://doi.org/10.1021/acs.organomet.5b00807.
[28] B.J. Eleazer, M.D. Smith, A.A. Popov, D.V. Peryshkov, (BB)-Carboryne complex of ruthenium: synthesis by double B–H activation at a single metal center, J. Am. Chem. Soc. 138 (2016) 10531–10538, https://doi.org/10.1021/jacs.6b05172.
[29] B.J. Eleazer, M.D. Smith, A.A. Popov, D.V. Peryshkov, Rapid reversible borane to boryl hydride exchange by metal shuttling on the carborane cluster surface, Chem. Sci. 8 (2017) 5399–5407, https://doi.org/10.1039/C7SC01846K.
[30] J.C. Smart, P.M. Garrett, M.F. Hawthorne, Novel σ-bonded transition metal carborane complexes, J. Am. Chem. Soc. 91 (1969) 1031–1032, https://doi.org/10.1021/ja01032a044.
[31] M.F. Hawthorne, D.A. Owen, Chelated biscarborane transition metal derivatives formed through carbon-metal σ bonds, J. Am. Chem. Soc. 93 (1971) 873–880, https://doi.org/10.1021/ja00733a012.
[32] H. Shen, Z. Xie, Constrained-geometry ruthenium carboranyl complexes and their unique chemical properties, Chem. Commun. (2009) 2431, https://doi.org/10.1039/b901549c.
[33] Z. Qiu, Z. Xie, Generation and reactivity of o-carborynes, Dalton Trans. 43 (2014) 4925–4934, https://doi.org/10.1039/c3dt52711e.
[34] L.E. Riley, A.P.Y. Chan, J. Taylor, W.Y. Man, D. Ellis, G.M. Rosair, A.J. Welch, I.B. Sivaev, Unprecedented flexibility of the 1,1′-bis(o-carborane) ligand: catalytically-active species stabilised by B-agostic B–H→Ru interactions, Dalton Trans. 45 (2016) 1127–1137, https://doi.org/10.1039/c5dt03417e.
[35] K.O. Kirlikovali, J.C. Axtell, A. Gonzalez, A.C. Phung, S.I. Khan, A.M. Spokoyny, Luminescent metal complexes featuring photophysically innocent boron cluster ligands, Chem. Sci. 7 (2016) 5132–5138, https://doi.org/10.1039/C6SC01146B.
[36] E.L. Hoel, M.F. Hawthorne, Preparation of B-σ-carboranyl iridium complexes by oxidative addition of terminal boron-hydrogen bonds to iridium(I) species, J. Am. Chem. Soc. 97 (1975) 6388–6395, https://doi.org/10.1021/ja00855a017.
[37] V.I. Bregadze, A.Y. Usiatinsky, N.N. Godovikov, Thallation of carboranes, J. Organomet. Chem. 292 (1985) 75–80, https://doi.org/10.1016/0022-328X(85)87322-8.
[38] L.M.A. Saleh, R.M. Dziedzic, S.I. Khan, A.M. Spokoyny, Forging unsupported metal–boryl bonds with icosahedral carboranes, Chem. Eur. J. 22 (2016) 8466–8470, https://doi.org/10.1002/chem.201601292.
[39] R.D. Adams, J. Kiprotich, D.V. Peryshkov, Y.O. Wong, Cage opening of a carborane ligand by metal cluster complexes, Chem. Eur. J. 22 (2016) 6501–6504, https://doi.org/10.1002/chem.201601075.
[40] W.-B. Yu, P.-F. Cui, W.-X. Gao, G.-X. Jin, BH activation of carboranes induced by late transition metals, Coord. Chem. Rev. 350 (2017) 300–319, https://doi.org/

10.1016/j.ccr.2017.07.006.
[41] Z.-J. Yao, W.-B. Yu, Y.-J. Lin, S.-L. Huang, Z.-H. Li, G.-X. Jin, Iridium-mediated regioselective B–H/C–H activation of carborane cage: a facile synthetic route to metallacycles with a carborane backbone, J. Am. Chem. Soc. 136 (2014) 2825–2832, https://doi.org/10.1021/ja4115665.
[42] Y. Quan, Z. Xie, Iridium catalyzed regioselective cage boron alkenylation of o-carboranes via direct cage B–H activation, J. Am. Chem. Soc. 136 (2014) 15513–15516, https://doi.org/10.1021/ja509557j.
[43] Y. Quan, Z. Xie, Palladium-catalyzed regioselective diarylation of o-carboranes by direct cage B–H activation, Angew. Chem. Int. Ed. 55 (2016) 1295–1298, https://doi.org/10.1002/anie.201507697.
[44] H. Lyu, Y. Quan, Z. Xie, Rhodium-catalyzed regioselective hydroxylation of cage B–H bonds of o-carboranes with O_2 or air, Angew. Chem. Int. Ed. 55 (2016) 11840–11844, https://doi.org/10.1002/anie.201605880.
[45] R.D. Adams, J. Kiprotich, D.V. Peryshkov, Y.O. Wong, Opening of carborane cages by metal cluster complexes: the reaction of a thiolate-substituted carborane with triosmium carbonyl cluster complexes, Inorg. Chem. 55 (2016) 8207–8213, https://doi.org/10.1021/acs.inorgchem.6b01403.
[46] Y. Quan, H. Lyu, Z. Xie, Dehydrogenative cross-coupling of o-carborane with thiophenes via Ir-catalyzed regioselective cage B–H and C(sp^2)–H activation, Chem. Commun. 53 (2017) 4818–4821, https://doi.org/10.1039/C7CC01485F.
[47] X. Wang, G.-X. Jin, Preparation, structure, and olefin polymerization behavior of a picolyl-functionalized carborane nickel(ii) complex, Organometallics 23 (2004) 6319–6322, https://doi.org/10.1021/om0493356.
[48] X. Wang, G.-X. Jin, Preparation, structure, and ethylene polymerization behavior of half-sandwich picolyl-functionalized carborane iridium, ruthenium, and rhodium complexes, Chem. Eur. J. 11 (2005) 5758–5764, https://doi.org/10.1002/chem.200500280.
[49] V. Terrasson, J.G. Planas, C. Viñas, F. Teixidor, D. Prim, M.E. Light, M.B. Hursthouse, Closo-o-Carboranylmethylamine–Pyridine associations: synthesis, characterization, and first complexation studies, Organometallics 29 (2010) 4130–4134, https://doi.org/10.1021/om1006374.
[50] R. Coult, M.A. Fox, W.R. Gill, P.L. Herbertson, J.A.H. MacBride, K. Wade, C-arylation and C-heteroarylation of icosahedral carboranes via their Copper(I) derivatives, J. Organomet. Chem. 462 (1993) 19–29, https://doi.org/10.1016/0022-328x(93)83337-u.
[51] F. Teixidor, A. Laromaine, R. Kivekäs, R. Sillanpää, C. Viñas, R. Vespalec, H. Horáková, Synthesis, reactivity and complexation studies of N, S exo -heterodisubstituted o-carborane ligands. Carborane as a platform to produce the uncommon bidentate chelating (pyridine)N-C-C-C-S(H) motif, Dalton Trans. 3 (2008) 345–354, https://doi.org/10.1039/B715362G.
[52] M.E. El-Zaria, K. Keskar, A.R. Genady, J.A. Ioppolo, J. McNulty, J.F. Valliant, High yielding synthesis of carboranes under mild reaction conditions using a homogeneous Silver(I) catalyst: direct evidence of a bimetallic intermediate, Angew. Chem. Int. Ed. 53 (2014) 5156–5160, https://doi.org/10.1002/anie.201311012.
[53] J.C. Axtell, K.O. Kirlikovali, P.I. Djurovich, D. Jung, V.T. Nguyen, B. Munekiyo, A.T. Royappa, A.L. Rheingold, A.M. Spokoyny, Blue phosphorescent zwitterionic iridium(iii) complexes featuring weakly coordinating nido-carborane-based ligands, J. Am. Chem. Soc. 138 (2016) 15758–15765, https://doi.org/10.1021/jacs.6b10232.
[54] E.S. Alekseyeva, A.S. Batsanov, L.A. Boyd, M.A. Fox, T.G. Hibbert, J.A.K. Howard, J.A.H. MacBride, A. Mackinnon, K. Wade, Intra- and inter-molecular carboranyl C–H···N hydrogen bonds in pyridyl-containing ortho-carboranes, Dalton Trans. (2003) 475–482, https://doi.org/10.1039/b209931d.
[55] E. Bosch, N.P. Bowling, J. Darko, The power of nonconventional phenyl C–H···N hydrogen bonds: supportive crystal-packing force and dominant supramolecular engineering force, Cryst. Growth Des. 15 (2015) 1634–1641, https://doi.org/10.1021/cg5014076.
[56] M.J. Martin, W.Y. Man, G.M. Rosair, A.J. Welch, 1,1′-Bis(ortho-carborane) as a κ2 co-ligand, J. Organomet. Chem 798 (1) (2015) 36–40, https://doi.org/10.1016/j.jorganchem.2015.04.011.
[57] L. Falivene, R. Credendino, A. Poater, A. Petta, L. Serra, R. Oliva, V. Scarano, L. Cavallo, SambVca 2. A web tool for analyzing catalytic pockets with topographic steric maps, Organometallics 35 (2016) 2286–2293, https://doi.org/10.1021/acs.organomet.6b00371.
[58] S.P. Fisher, A. El-Hellani, F.S. Tham, V. Lavallo, Anionic and zwitterionic carboranyl N-heterocyclic carbene Au(I) complexes, Dalton Trans. 45 (2016) 9762–9765, https://doi.org/10.1039/c6dt00551a.
[59] K. Hermansson, M. Wójcik, S. Sjöberg, O- ,m-, and p-carboranes and their anions: ab initio calculations of structures, electron affinities, and acidities, Inorg. Chem. 38 (1999) 6039–6048, https://doi.org/10.1021/ic990381l.
[60] V. Kalinin, V. Ol'shevskaya, Some aspects of the chemical behavior of icosahedral carboranes, Russ. Chem. Bull. 57 (2008) 815–836, https://doi.org/10.1007/s11172-008-0120-x.
[61] S.S. Rozenel, J.B. Kerr, J. Arnold, Metal complexes of Co, Ni and Cu with the pincer ligand $HN(CH_2CH_2P^iPr_2)_2$: preparation, characterization and electrochemistry, Dalton Trans. 40 (2011) 10397–10405, https://doi.org/10.1039/C1DT10599J.
[62] B. Vabre, Y. Canac, C. Lepetit, C. Duhayon, R. Chauvin, D. Zargarian, Charge effects in PCP pincer complexes of Ni^{II} bearing phosphinite and imidazol(i)ophosphine coordinating jaws: from synthesis to catalysis through bonding analysis, Chem. – Eur. J. 21 (2015) 17403–17414, https://doi.org/10.1002/chem.201502491.
[63] D.F. Shriver, M.A. Drezdzon, The Manipulation of Air-sensitive Compounds, second ed., Wiley-Interscience, New York, 1986, 2 edition.
[64] APEX3, Bruker AXS, Inc., Madison, Wisconsin, USA, 2016.
[65] SAINT+, Bruker AXS, Inc., Madison, Wisconsin, USA, 2016.
[66] L. Krause, R. Herbst-Irmer, G.M. Sheldrick, D. Stalke, Comparison of silver and molybdenum microfocus X-ray sources for single-crystal structure determination, J. Appl. Crystallogr. 48 (2015) 3–10, https://doi.org/10.1107/S1600576714022985.
[67] G.M. Sheldrick, A short history of SHELX, Acta Crystallogr. A 64 (2008) 112–122, https://doi.org/10.1107/S0108767307043930.
[68] G.M. Sheldrick, SHELXT – integrated space-group and crystal-structure determination, Acta Crystallogr. Sect. Found. Adv. 71 (2015) 3–8, https://doi.org/10.1107/S2053273314026370.
[69] O.V. Dolomanov, L.J. Bourhis, R.J. Gildea, J. a. K. Howard, H. Puschmann, OLEX2: a complete structure solution, refinement and analysis program, J. Appl. Crystallogr. 42 (2009) 339–341, https://doi.org/10.1107/S0021889808042726.